Applied Energy 185 (2017) 1362–1371

Contents lists available at ScienceDirect

Applied Energy

journal homepage: www.elsevier.com/locate/apenergy

Ammonia–methane combustion in tangential swirl burners for gas turbine power generation

Agustin Valera-Medina [a,*], Richard Marsh [a], Jon Runyon [a], Daniel Pugh [a], Paul Beasley [b], Timothy Hughes [b], Phil Bowen [a]

[a] Cardiff University, Cardiff, Wales, UK
[b] Siemens PLC, Oxford, England, UK

HIGHLIGHTS

- Ammonia can become a new energy vector for large scale power generation.
- Ammonia fuelled gas turbines have been barely studied. Scarce literature exist.
- Current research provides findings that show NH_3 potential as gas turbines fuel.
- Unfortunately, weak flame stability and high emissions are still restrictive.
- Stratified injection with low swirl might be the best way to use these blends.

ARTICLE INFO

Article history:
Received 23 July 2015
Received in revised form 10 February 2016
Accepted 14 February 2016
Available online 24 February 2016

Keywords:
Ammonia
Gas turbines
Swirling flows

ABSTRACT

Ammonia has been proposed as a potential energy storage medium in the transition towards a low-carbon economy. This paper details experimental results and numerical calculations obtained to progress towards optimisation of fuel injection and fluidic stabilisation in swirl burners with ammonia as the primary fuel. A generic tangential swirl burner has been employed to determine flame stability and emissions produced at different equivalence ratios using ammonia–methane blends. Experiments were performed under atmospheric and medium pressurised conditions using gas analysis and chemiluminescence to quantify emission concentrations and OH production zones respectively. Numerical calculations using GASEQ and CHEMKIN-PRO were performed to complement, compare with and extend experimental findings, hence improving understanding concerning the evolution of species when fuelling on ammonia blends. It is concluded that a fully premixed injection strategy is not appropriate for optimised ammonia combustion and that high flame instabilities can be produced at medium swirl numbers, hence necessitating lower swirl and a different injection strategy for optimised power generation utilising ammonia fuel blends.

1. Introduction

In 2013, the UK Government released an Energy Bill that requires a massive decarbonisation of the power sector by 2030, with the emissions intensity rapidly reduced, and a new generation of clean power plants to be built. This will ensure the UK can cut its greenhouse gas emissions by 50% in 2025. A potential enabler for this low carbon economy is the energy vector 'Hydrogen'. However, issues associated with storage and distribution are currently a barrier to its implementation. Ammonia has been suggested as a substitute of hydrogen – for mobile and remote applications – being a carbon free carrier that offers an energy density close to some fossil fuels. However, further detailed understanding of the combustion process, emissions production and combustion stabilisation using this gas for power generation are still the main barriers for its usage as a fuel within industrial gas turbines.

Similar to synthesised hydrogen, ammonia is a product that can be obtained either from fossil fuels, biomass or other renewable sources [1]. Some advantages of ammonia with respect to hydrogen are its lower cost per unit of stored energy, higher volumetric energy density, easier production, handling and distribution, and better commercial viability [2]. Ammonia has a narrow flammability range and is therefore generally considered non-flammable when transported. If released into the atmosphere, its density is lighter than that of air and thus dissipates rapidly [1,3]. However,

* Corresponding author. Tel.: +44 (0) 2920 875948.
E-mail address: valeramedinaa1@cardiff.ac.uk (A. Valera-Medina).

http://dx.doi.org/10.1016/j.apenergy.2016.02.073
0306-2619/

there remain considerable challenges including mitigation of the potential for considerable NO production, as well as hazard management in terms of the chemicals high levels of toxicity.

Ahlgren [4] performed a study, comparing the fuel power density F (TW/m^2, a unit that takes into consideration the power in the fuel and the energy required to transport it in pipelines) of different fuels, showing that ammonia and methanol are the best renewable fuels if compared with pure hydrogen. Ammonia can be stored in the same manner as propane at 8 bar vapour pressure at room temperature, thus making it a good candidate for affordable, low-carbon power generation if produced using alternative sources [5–9]. However, the required technology to deliver this so-called "green NH_3 fuel" vision has been only demonstrated at comparatively small scale using internal combustion engines and fuel cells. Therefore, the way forward requires its implementation into gas turbines to partially replace fossil fuels across the globe for greater low-carbon power generation, thus integrating the technology within the complete energy cycle.

Considerable research has taken place to develop technologies capable of burning the fuel in gas turbines since the 1960s [10–12]. It was found through experimental studies that the minimum ignition energy of ammonia was 16 times higher than for fossils. At stoichiometric conditions, the quenching distance for ammonia–air was 3.5 greater than for propane, with ammonia burning at only one-half the bulk flow velocity possible with hydrocarbon fuels with a narrower equivalence ratio range [11]. Experiments at 28% dissociated ammonia showed similar properties to those using hydrocarbons. It was concluded that 28% dissociated ammonia could be used as a substitute fuel in gas turbine combustion systems optimally sized for hydrocarbon fuels – although the additional chemical energy and timescales for this dissociation must be considered. Other experiments demonstrated that the fundamental problem with ammonia–air as a turbine fuel is the relatively slow chemical reaction rate, giving a laminar burning velocity of ~6–8 cm/s [13]. As air flow is reduced to allow sufficient residence time for the reaction to progress, diminished Reynolds number effects lead to less turbulence and hence less effective mixing. This in turn decreases combustion efficiency [12]. Other studies [14–16] showed that another problem with the use of ammonia in combustion systems is the high production of NO_x emissions. Whilst reduction of thermal and prompt NO_x are always a challenge in gas turbine combustion, the use of ammonia as a fuel significantly increases the likelihood of fuel-bound nitrogen reacting with oxygen. Toxicity is also a significant safety consideration [17].

In experimental studies, Solar and UC Berkeley used a 250HP T-350 single can burner turbine to run experiments in the 1960s [18]. Performance of a T-350 engine with ammonia was comparable to the performance with JP-4, with tests only limited to ammonia in the vapour phase. Ammonia at 2.35 times the mass flow of hydrocarbon fuels provided cooler turbine inlet temperatures, with an increase of 10–20% when temperatures were matched. More recently, a number of different approaches have been followed to use ammonia as a flexible fuel in gas turbines. Karabeyoglu et al. [19] present some important issues of using NH_3, arguing that toxicity and low energy density are the major problems. In 1991, the Italian power generator ENEL undertook a research program on gas turbine challenges associated with flexibility using gaseous blends that included ammonia, citing emissions as the biggest problem [20]. Grcar et al. [21] combined experimental and modelling investigations of ammonia chemistry in a hot combustion environment that was below adiabatic flame temperatures, such as those observed in post combustion gases. The final products of NH_3 oxidation remained sensitive to mixing even at temperatures below those of self-sustaining flames. At low temperatures, NH_3 oxidation occurred in a premixed reaction zone, but at sufficiently high temperatures a non-premixed reaction zone that produces significantly less NO than the equivalent premixed system developed.

Although research has been undertaken for operational flame limits, chemical models, flame speed and internal combustion engines, gas turbines have played a minor role using this fuel. Groups that have shown some development on the understanding of these systems are limited [16,18,22,23]. To the best knowledge of the authors, SPG Advanced Propulsion and Energy [18,19] are the only company claiming developments close to commercialisation. Their findings show how higher mass flow rates are required to achieve similar power outputs if compared to methane, but at the same time the outlet temperatures are lower. They also presented a series of challenges when using this technology: (a) lower flame temperatures and slower kinetics; (b) stable, efficient combustion with liquid NH_3 is problematic, thus additives should be used; (c) ammonia can be burned in combustors in the vapour phase, thus there is a need to develop systems capable of vaporising ammonia; (d) cracking of the molecule can produce great advantages and increase flame speed and burning ratios. NASA also identified during their XLR-99 program the need for "combustor enhancers" such as hydrogen, gasoline, kerosene, and propane, especially during start-up and idle [23].

Swirl stabilised combustion of ammonia with other molecules has briefly been analysed by Meyer et al. [22] in a 40 kW burner, with nozzles, swirl stabilisers and a self-sustained heat exchanger. Stabilisation was achieved using different swirlers with different concentrations of ammonia, hydrogen and methane. For those experiments where ammonia and hydrogen were mixed, it was found that the use of a flame holder increased the combustion efficiency, with a demonstrable reduction in NO_x emissions. Japanese researchers have also started to play an important role in the development of new ammonia systems. The Fukishima Renewable Energy Institute (FREA), is developing a new fuel flexibility platform to burn liquid ammonia from wind and solar energy combined with kerosene in a 50 kW micro-gas turbine [24]. It has been demonstrated that the equipment can be run using ammonia–kerosene blends at different concentrations. However, the production of NO_x increases considerably based on the amount of ammonia injected, reaching levels of up to 600 ppmV. Other potential beneficiaries of the research undertaken include the steel industry whereby ammonia is currently available and could be considered as fuel to be co-fired in *low-pressure* furnaces, as considered in this study.

It is clear that a considerable gap exists between the growing interest in ammonia-based power applications, current knowledge and understanding required to inform optimum designs. In particular, the fuel mixture blends and injection strategies which optimise the emission and stability performance of practical swirl combustors are poorly understood. Hence, the aim of this paper is to provide a first insight into these practical issues, utilising a premixed generic burner and practically-relevant swirl-number, investigating ammonia/methane blends. A preliminary investigation into the influence of raised ambient conditions is also explored for gas turbine applications. Hence, this paper helps to bridge the gap between research, development and implementation for an innovative technology which has the potential to provide a sustainable energy system. Both experimental and modelling tools are utilised to derive conclusions and provide informed guidance.

2. Experimental and model setup

Experiments were performed at the Gas Turbine Research Centre (GTRC) which is a Cardiff University facility [25]. Its rigs are designed for the study of different facets of the combustion process

and are operated at different pressures. One of these rigs, the High Pressure Optical Chamber (HPOC) rig is capable of burning up to 5 different fuels simultaneously. For the current project, the HPOC rig was fitted with a generic premixed swirl burner, Fig. 1. The generic swirl burner consists of a main body that receives both the premixed (air and fuel) gases and a lance that is used for liquid injection, not used in these tests. The entire rig is confined by a quartz tube fitted to the system to provide a confinement for the flame, as utilised in modern gas turbine combustors. Coriolis mass flow meters were used to achieve precise measurement of flowrates with an accuracy of ±0.5% RD plus ±0.1% FS. Further information can be found in previous works [26].

Different equivalence ratios, Reynolds numbers and ammonia/methane fuel concentrations were investigated using a geometric swirl number of 1.05. Re varied from 10,800 to 21,000 for a range of operating conditions, shown in Table 1. It must be emphasised that only one of the tested blends was successfully characterised, i.e. 61% NH_3–39% CH_4 by molar fraction. Pure ammonia and blends with ~10% methane were impossible to ignite and operate. Blends with ~20% and ~30% CH_4 showed impracticably unsteady behaviour, especially under close to stoichiometric conditions. Therefore, a mixture close to 60–40% was attempted based on previous experimental campaigns (tests to be published). It must be emphasised that higher power conditions could improve the response of blends with lower methane concentrations; however, the current setup only allowed for ammonia mass flowrates up to 0.8 g/s. Herein, only two power conditions at atmospheric pressure were considered, as shown in Table 1. Pressurised tests were performed using 45.0 g/s of bypass air over the combustion chamber (but separated from the combustion zone by the quartz tube) to provide sufficient overall flow to raise the pressure to 2 bar (absolute). A 30 kW power load was studied under these conditions. An Avigilon 5 Mp H.264 HD camera was used to capture the flame during various stability stages and provide qualitative insights of the flame behaviour.

OH* chemiluminescence was used on all the blends. The chemiluminescence intensity of the OH radical is low and requires the use of an image intensifier to capture the light emitted in the UV range. A Dantec Dynamics Hi Sense Mk II CCD camera with a 1.3 megapixel resolution was coupled to a Hamamatsu C9546-03L image intensifier. A specialty 78 mm focal length lens (F-stop = f/3.8) capable of capturing light in the UV wavelength range was installed on the image intensifier along with a narrow band pass filter centred at 307 nm (FWHM = 10 nm). Two hundred OH* chemiluminescence images were taken at 10 Hz at each test condition using Dantec's Dynamic Studio software, whilst the image intensifier gain was controlled via remote control. All images were taken through the top window of the HPOC at a 90° angle to the direction of flow. A bespoke Matlab program was developed to determine the Centre of Gravity (CoG) of the OH* chemiluminescence intensity images [27,28], herein giving insights of the average movement of the flame. CoG is given by,

$$\mathrm{CoG} = \left[\frac{\sum_{i,j} i \cdot I(i,j)}{\sum_{i,j} I(i,j)}, \frac{\sum_{i,j} j \cdot I(i,j)}{\sum_{i,j} I(i,j)}\right] \quad (1)$$

where $I(i,j)$ is the OH* intensity function. Using this method the centre of gravity is attracted by those regions with higher intensity pixels. The background was subtracted from the raw images to give weight only to OH* radical zones.

Two pieces of equipment were used to characterise combustion emissions, the first is an integrated system developed by Signal Instruments comprising several analysers: A Flame Ionisation Detector (FID) is employed within a Signal 3000HM to detect Total Hydrocarbons (THCs), calibrated with propane in the range 0–890 ppm. A heated vacuum chemiluminescence analyser (Signal 4000VM) is simultaneously employed to quantify NO_x concentrations, calibrated to 37.1 ppm NO and 1.9 ppm NO_2. The system also contains a multi-gas analyser (Signal MGA), containing an infrared cell for measurement of CO (calibrated for 0–900 ppm) and CO_2 (0–9%), in addition to a paramagnetic O_2 sensor (up to 22.5%). A system for quantifying trace concentrations of NH_3 in the flue gas was used during the medium pressure tests, and forms a subsystem to the 4000VM NO_x analyser. As a backup and for data confidence, a standalone Rosemount NGA 2000 multi-gas analyser, and provides secondary readings of CO, CO_2 and O_2 all calibrated to the same concentrations previously stated. Equipment calibration showed a ~5% measurement error.

Chemical, 0-D equilibrium calculations were performed using the software GASEQ. Fundamentals of the program are based on complex, balanced chemical calculations defined by Sanford Gordon and Bonnie J. McBridge for NASA [29]. Here the products calculation is performed through the resolution of the free energy equation for n species,

$$\frac{G}{RT} = \sum_{i=1}^{nSp}\left(\frac{x_i G_i^0}{RT} + x_i \ln\frac{x_i}{\sum x_i} + x_i \ln p\right) \quad (2)$$

Finally, CHEMKIN-PRO was used to model the progression of different critical species and radicals through a 1-D combustion chamber. A hybrid Perfectly Stirred Reactor–Plug Flow Reactor

Table 1
Experimental matrix at 61% NH_3 and 39% CH_4.

	MASS NH_3 [g/s]	MASS CH_4 [g/s]	MASS O_2 [g/s]	MASS AIR [g/s]	Base POWER [KW]	STOICH.
	1.0 bar (absolute)					
1	0.58	0.34	2.56	11.73	31.84	0.84
2	0.58	0.34	2.10	9.48	31.75	1.04
3	0.58	0.34	1.73	7.84	31.86	1.26
4	0.58	0.34	1.66	7.54	31.70	1.31
5	0.58	0.34	1.56	7.06	31.79	1.38
6	0.58	0.34	1.49	6.75	31.71	1.46
7	0.80	0.47	3.68	16.66	43.85	0.81
8	0.82	0.47	2.93	13.25	44.30	1.02
9	0.82	0.47	2.62	11.88	44.30	1.14
10	0.82	0.47	2.40	10.86	44.30	1.24
11	0.80	0.47	2.18	9.85	43.85	1.37
	2.0 bar (absolute)					
12	0.58	0.34	2.73	12.35	31.75	0.80
13	0.58	0.34	2.10	9.57	31.75	1.03
14	0.58	0.34	1.91	8.65	31.75	1.14
15	0.58	0.34	1.77	8.00	31.75	1.23
16	0.58	0.34	1.54	6.98	31.75	1.42

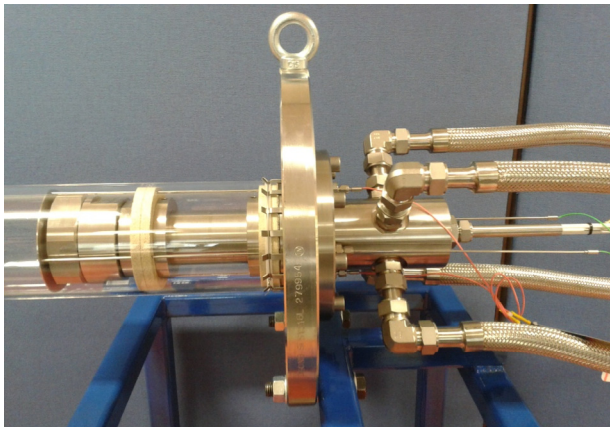

Fig. 1. Generic swirl burner.

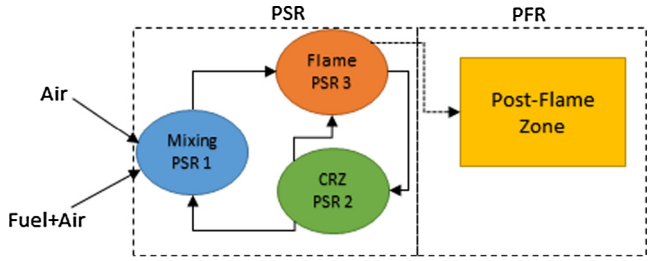

Fig. 2. PSR–PFR schematic.

Fig. 3. Flame with an ammonia–methane blend. Equivalence ratio 1.31, point 4 Table 1. Flow is left-to-right.

(PSR–PFR) network was utilised for the most stable conditions at 1 and 2 bar (absolute), test points 9 and 15 in Table 1. This type of network is commonly used to simulate mixing and flow characteristics in gas turbine combustors [30]. The reactor network has two clusters. The first cluster represents the swirling flame with a central recirculation zone (CRZ) [31] whose recirculation was set at 20% of the product gases. Recirculation strength was approximated from previous experimental campaigns using similar burners [32,33]. The second cluster uses a single Plug Flow Reactor for post-flame processes along a 0.1 m duct. A schematic of the network is presented in Fig. 2. The analysis was performed using Konnov's mechanism [33–36]. Reaction pathways are presented in different sections of the network to show the evolution of important species through the combustion process.

3. Results and discussion

Ignition was achieved using pure methane at a flowrate of 0.4 g/s with a 1 J spark ignition, primarily for safety and operational reasons. The flow rate of Ammonia was increased until the desired blend specified in Table 1 was achieved. During transition, the flame did not show any major stability change up to an equivalence ratio of 1.0. It was above stoichiometric conditions that visible light intensity at the crown of the flame was more energetic, with a continuous increase towards an orange, more efficient combustion zone product of more NH_2 radicals and H_2O [37]. Once the fuel mass flow had reached the specific power conditions, the air flow rate was decreased to evaluate the influence of different equivalence ratios.

The combustion process denoted methane burning features close to the burner nozzle under lean conditions with an elongated stable flame crowned by an unstable, highly wrinkled zone where the ammonia was reacting. It was evident that under stoichiometric conditions the system started to experience combustion instabilities triggering an axial, vibrating displacement of an even more wrinkled flame. As the air flowrate was decreased further, the flame became more unstable, with considerable vibration in its core and crown. Further increase in the equivalence ratio to ϕ = 1.31 showed an unstable flame with corrugation across the flame, with a wider, larger crown where most of the ammonia was being burnt, Fig. 3.

Emission analyses showed clear correlations between trends obtained during the experiments and those predicted using 0-D calculations, especially for NO_x, CO, CO_2 and O_2, Fig. 4. However, the software exhibited considerable under-prediction for the fuel species, i.e. CH_4 and NH_3. Since the model assumes that the reaction takes place as a balance between all reactants, the results indicate that fuels are completely consumed with further decrease in oxygen content than during experimental trials. This excess of fuel in the simulation denotes a less efficient combustion process with a clear over-prediction of CO and reduced CO_2 to the one obtained experimentally. NO_x are also reduced as a consequence of this drop in efficiency linked to lower combustion temperatures. Although the experiments showed high traces of unburned fuel, it is believed that for the fuel that did burn the process was more efficient as a consequence of the presence of recirculatory zones that anchor the flame whilst increasing recirculation of reacting gases [38]. Therefore, it seems clear that the injection strategy is not adequate with considerable amounts of unburnt fuel. On the other hand, the presence of coherent structures can increase combustion efficiency by increasing the residence time of a kinetically slow fuel such as ammonia.

Numerical and experimental results indicate that rich combustion around 1.14 and 1.25 equivalence ratio produces the lowest incomplete combustion species, i.e. CO, THC and unburned NH_3, though CO levels in particular are still unacceptably high. Whilst this sounds counter-intuitive, it should be borne in mind that significant quantities of unburnt products were produced at lean conditions, whereas in methane–air combustion this would provide almost complete oxidation. It is under this condition that NO_x emissions were also considerably decreased to levels below 30 ppm, Fig. 4. It is evident that the process improves with the increase of pressure, a phenomenon expected as a consequence of higher interaction between molecules, compacted coherent flow structures and faster flows. CO_2 and O_2 were not documented at higher pressures since the by-pass flow (which is mixed with the core combustion flow products far downstream) overwhelmed the values obtained inside of the combustion chamber, making them difficult to read at very low (highly diluted) concentrations.

1-D numerical simulations were conducted under these rich conditions, point 9 and 15 in Table 1, Fig. 5. Solutions indicate the gas ignition occurs in the flame zone (PSR 3) with an increase of temperature in the recirculation zone (PSR 2) where CH_4, NH_3 and some H_2 keep reacting. It is also clear that in the flame zone H_2 has been produced accompanied by the production of NH_2 and OH radicals that keep reacting with further increase of temperature. More CO has been produced than CO_2 as a consequence of oxygen depletion. Increasing pressure, Fig. 5B, shows a slight rise in temperature from 2180 K to 2230 K accompanied by a minor reduction of H_2 and a greater decay in OH and NH_2 radicals as a consequence of an increment in the amount of reactions. Combustion improves by the recirculation of OH and NH_2. The model also over-predicts the reaction of all fuel producing more incomplete combustion species, as opposed to the experimental data.

The reaction pathway provided more insights of the evolution of ammonia in this flow, Fig. 6. Most ammonia reacts to form water, hydrogen or NH_2. The latter keeps reacting with OH to form even more water. From Konnov's mechanism [36], NO_x seem to be a product mainly generated from the interaction between NH and N with oxygen, as well as the reaction $HNO + H \rightarrow NO + H_2$. Experiments showed similar flame trends to those obtained numerically with the reaction of NH_2 and production of water, denoting an orange flame [37] and visible deposits of condensed water after

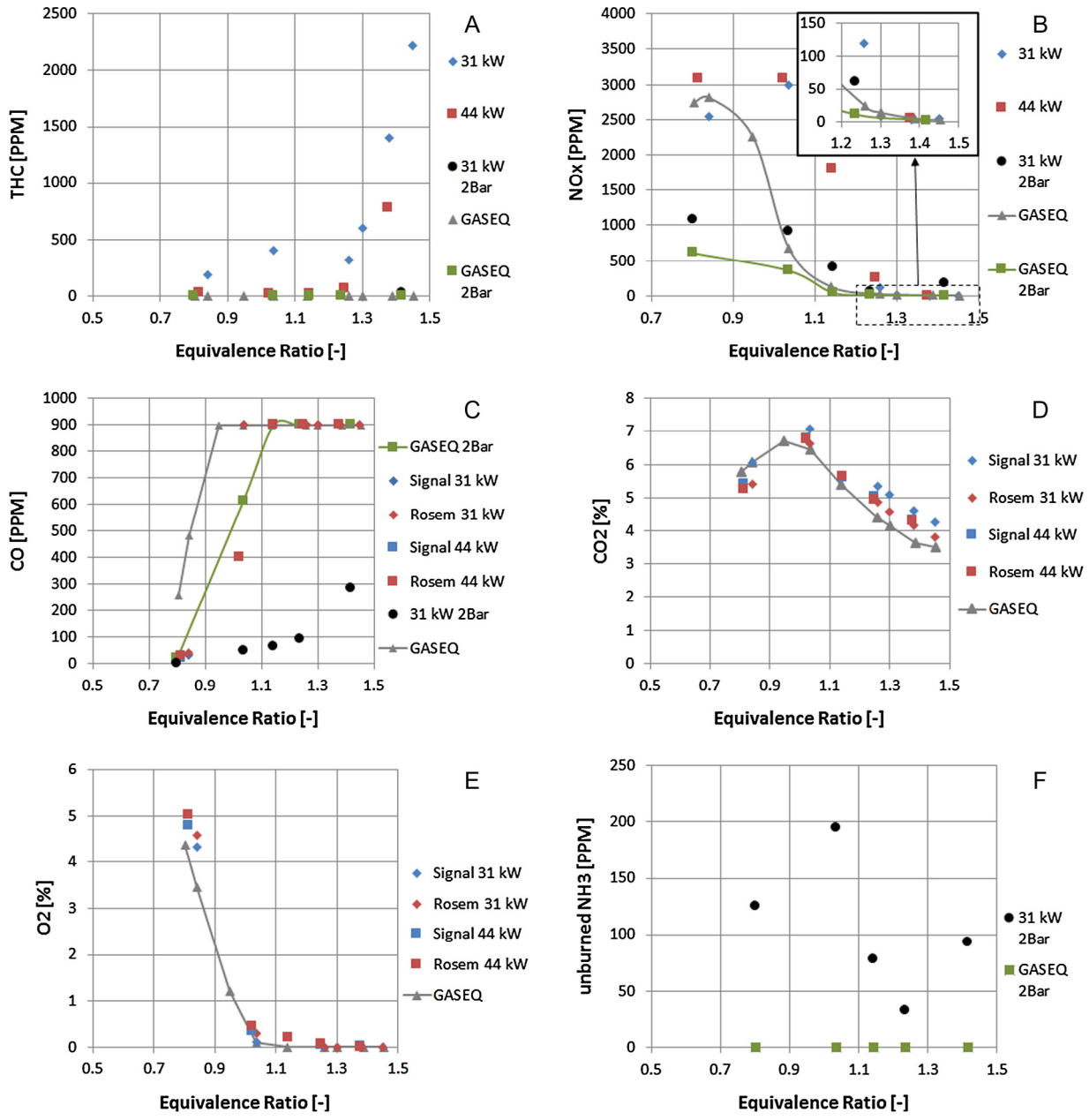

Fig. 4. Emissions measurements (experimental) and Equilibrium predictions. CO, CO_2 and O_2 scaled to dry conditions.

each trial, respectively. However, it is again clear that experimentally the process was not as efficient as in the simulation predicts. Experiments indicated a methane flame close to the burner mouth, thus augmenting OH along the flame and depleting oxygen. Correlating with the 1-D simulation, hot ammonia starts to crack, a phenomenon observed further downstream at the end of the flame. High interaction with the remaining oxygen and reactants produces even more OH radicals that will react with H_2 to form water. Therefore, the upstream methane flame provides the heat needed to start the reaction of ammonia and production of OH and NH_2 further downstream.

Further analyses in the post-flame region indicate a rise in temperature as a consequence of the reaction of OH, CO, NH_2 and NO, Fig. 7. OH radicals are a highly active species at the beginning of the post-flame region reacting with hot H_2. NO_x reacts along the post-flame reactor providing oxygen to form more OH or O radicals that can interact with CO to produce CO_2. The former mechanism seems to be linked to the chemical effect of the remaining NH_2 produced through the reaction $NH_2 + NO \rightarrow N_2H + OH$ [33,39]. Sources of oxygen for CO are obtained from the formed OH or the reaction $N + NO \rightarrow N_2 + O$ [39].

The 1-D simulation under-predicts the unburnt fuel species and also over-predicts CO, showing that the mixing appears to be less than required for fully premixed conditions. On the other hand, the results also emphasise that if this was the case, a fully premixed flame is not suitable for this blend at the proposed inlet conditions. However, NO_x reduction is a phenomenon that shows good correlation between modelled and experimental data, and this occurs in the post-flame region with the increase of OH and H_2. These findings lead to the postulation of a need for more effective injection geometries with further fluidic stabilisation downstream of the combustion zone to oxidise these highly reactive species more effectively.

During the experimental campaign, it was under rich conditions that the flame started to display signs of considerable instability. Images were obtained to qualitatively denote the vibration and

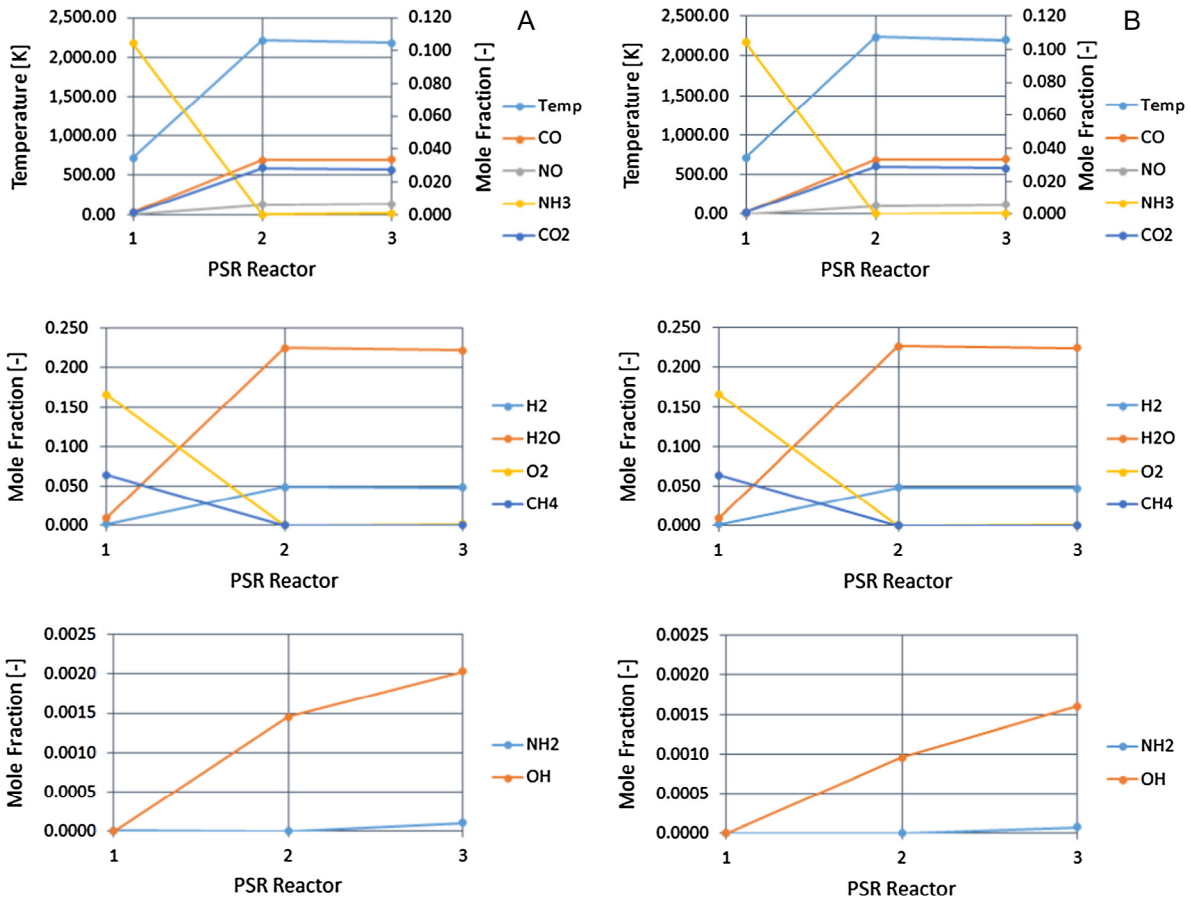

Fig. 5. 1-D Simulation in the PSR reactions using a swirling network. (A) Atmospheric conditions, point 9, Table 1; (B) medium pressurised conditions, point 15, Table 1.

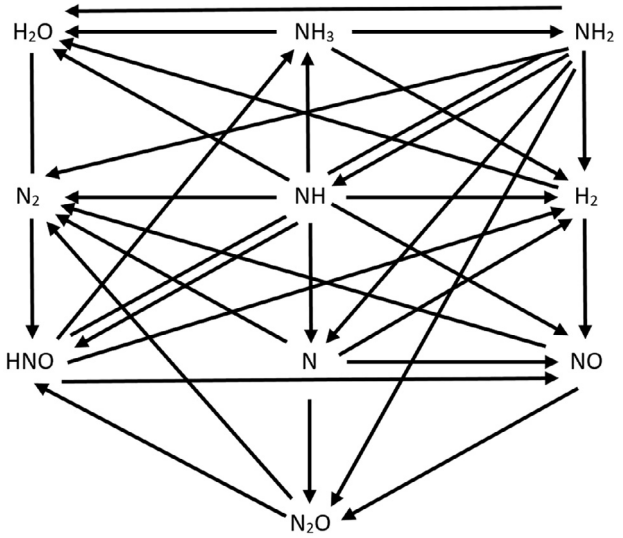

Fig. 6. Reaction paths of ammonia in the flame zone.

change of the central recirculation zone (CRZ) [33], Fig. 4, at different times through the experiments, Fig. 8. It is clear that the size of the inner region of the flame has decreased, whilst the crown has widened. This change has a direct impact on the combustion phenomenon causing a series of thermoacoustic instabilities [40,41] that are not detailed in this work.

A more detailed, quasi-quantitative study was performed using OH* Chemiluminescence, Figs. 9–11. Results showed both a minimum and maximum standard deviation of 4.3% and 15.0% of the total intensity range, respectively. Minimum values were observed close to the burner nozzle whilst the largest fluctuations appeared at the front end of the flame. Fig. 9A shows a comparison between cases at various equivalence ratios. Results were normalised to the value obtained using lean, atmospheric conditions, Fig. 9B. As the equivalence ratio is increased the production of OH* radicals decreases. However, the flame shows a peak production at 1.23 equivalence ratio. This is linked to the reaction path $NH_2 + NO \rightarrow N_2H + OH$ which has been enhanced. During the experimental programme, there was evidence that a shift in the combustion process took place, moving from a methane-driven to an ammonia-driven series of reactions. It is proposed that once the flame reaches a point just above 1.15 equivalence ratio, higher flame temperatures increase the cracking of ammonia and NO_x production. This triggers a greater recombination of NH_2 with nitrogen oxides, thus reducing the latter and increasing OH* emissions, as observed. Moreover, NO_x formation is limited due to the lack of oxygen, which also decreases the total concentration of these molecules. It appears that it is at this condition that fuel reactions between air–methane and air–ammonia reach a balance in reactivity. From this point onwards, flame temperatures reduce and NH_3 has a more active interaction with NO than CO with the remaining oxygen, if any. Further research is required to substantiate this plausible hypothesis.

Results for CoG show the axial asynchronous displacement of the flame accompanied by its radial oscillation, Fig. 10A. This is a methodology followed by other authors [27] that showed promising results to determine the movement of grey bodies as those obtained in this work. Similarly, analyses of OH* production denoted the variance of this radical in time, Fig. 10B. An arbitrary,

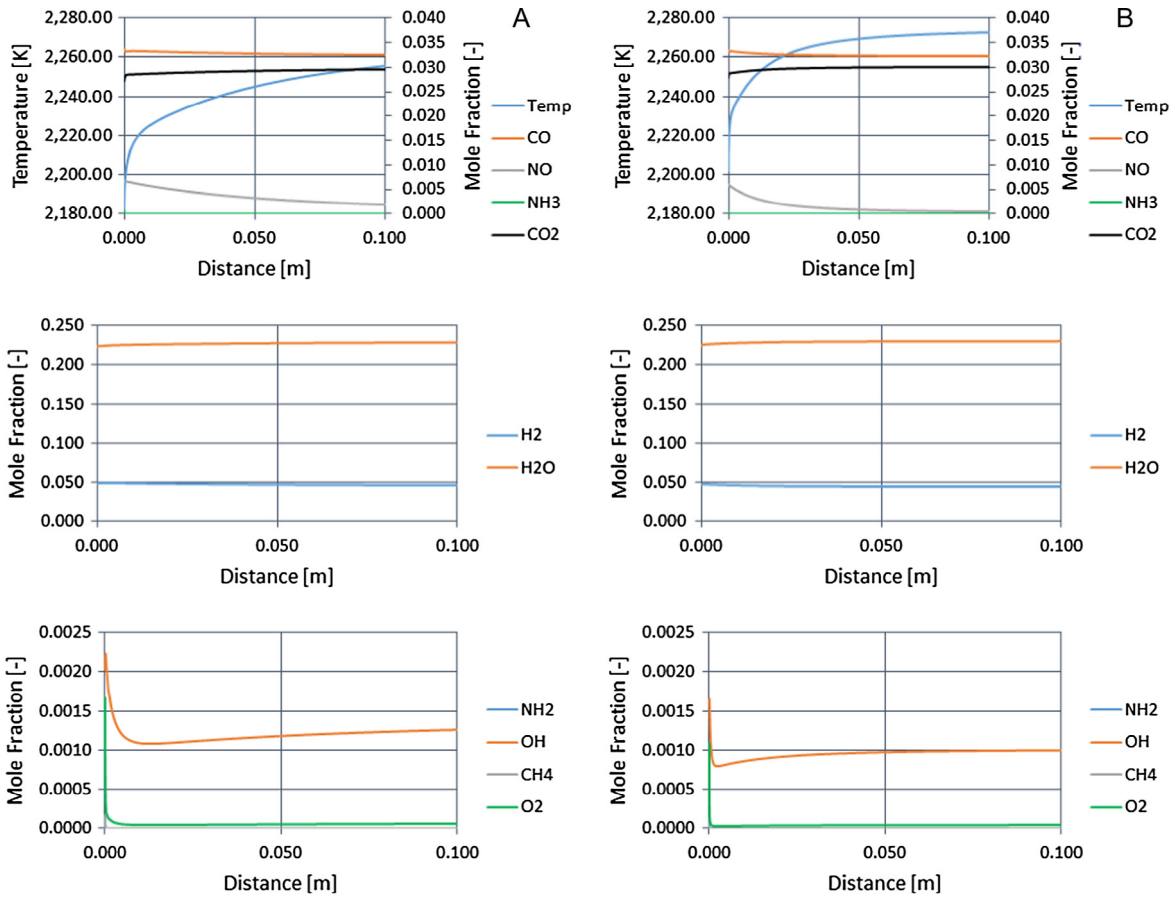

Fig. 7. 1-D Simulation in the PFR reactor using a swirling network. (A) Atmospheric conditions, point 9, Table 1; (B) medium pressurised conditions, point 15, Table 1.

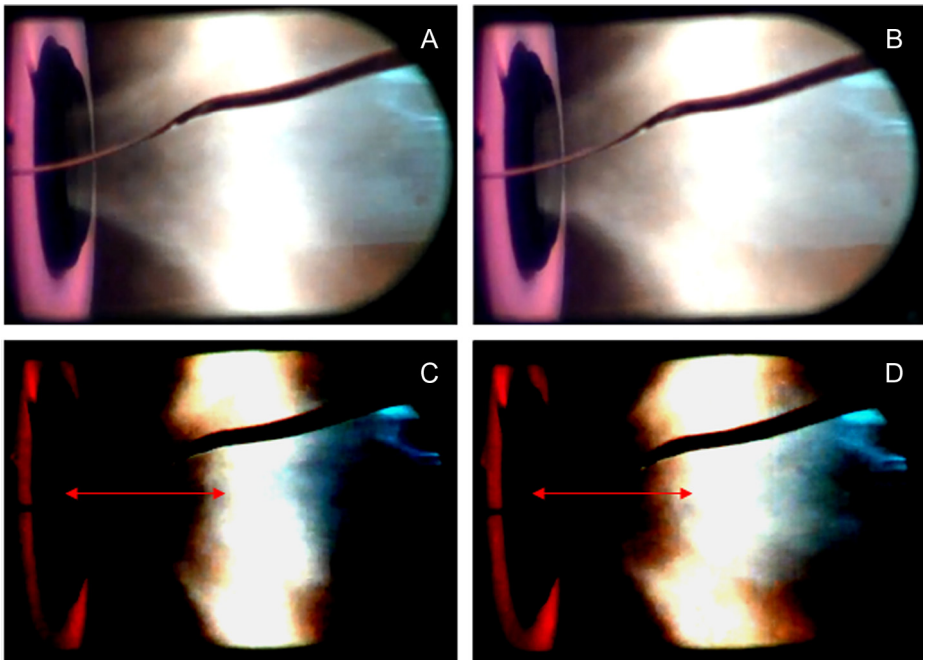

Fig. 8. Instantaneous photographs. (A and B) Original. (C and D) Modified at −50% brightness and 65% contrast. Axial initial position of crown as in C, denoted by arrow. Clear displacement and flame change between C and D. The diagonal mark in the image is a surface crack in the quartz flame holder, which did not affect the results.

starting measuring point was defined at $t = 0.0$ s. It is recognised that radial oscillations are caused by highly 3-dimensional flame structures [42]. However, the axial displacement seems to be caused by another process. It is believed that the process is as follows: oxygen starts to burn with methane in the shearing flow close to the burner mouth, producing OH. OH radicals and some

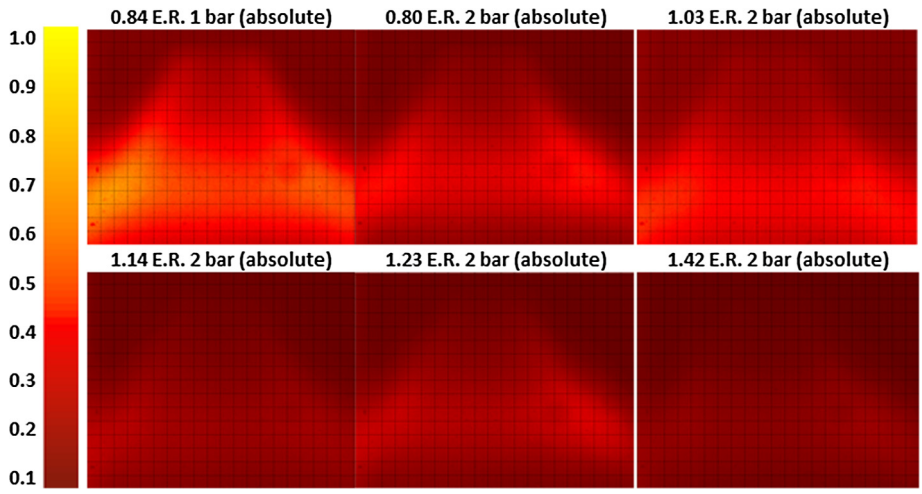

Fig. 9. (A) OH* chemiluminescence, mean values from 200 images; (B) normalised intensity of mean values using results at 0.84 E.R. at 1 bar (absolute).

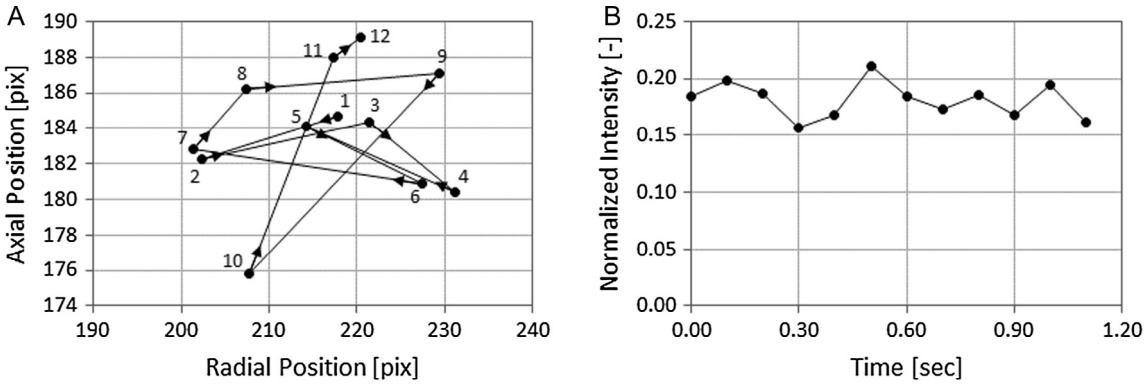

Fig. 10. (A) OH* CoG; (B) normalised OH* Intensity. Norm as at 0.84 E.R. at 1 bar.

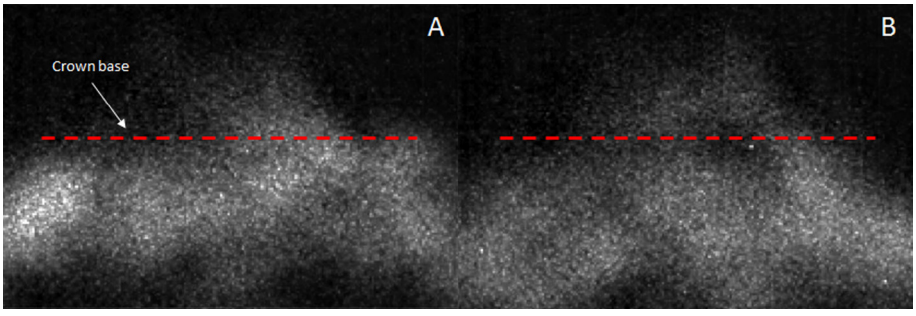

Fig. 11. Difference in OH* profiles for the same flame at (A) 0.9 s, point 10 Fig. 10(A); and (B) 1.1 s, point 12 Fig. 10(A).

O_2 are confined within the strong CRZ and continue reacting with the CO and newly formed species from the ammonia cracking located at the crown base, Fig. 11A. This process can be observed as the OH* CoG is pulled closer to the burner mouth, Fig. 10A points 8–9. The reaction produces a sudden expansion of the CRZ with a reduction in recirculation pushing the flame downstream, Fig. 10A point 10. The lack of oxygen and lower reactivity in this weaker CRZ shrinks the CRZ and brings the flame closer to the nozzle, Fig. 10A points 11–12. This reduction is accompanied by movement of ammonia into the recirculation zone. From that point, the lower reactivity of the ammonia reduces the flame speed and pushes back the flame to its original position, re-establishing its initial conditions, herein restarting the process. Although it is recognised that faster measuring techniques are required to provide more details of the phenomenon, the results provide clear guidance on further works on this topic. Other works with methane flames [41] have demonstrated that thermo-acoustic instabilities trigger a cycle where pressure oscillations produce fuel injection variation and mixing problems at the burner mouth, with swirl number waves that change the size and strength of the central recirculation zone. These phenomena are not excluded from the present results, and it is recognised that more research needs to be done in order to observe these impacts on ammonia blend flames.

Although the CRZ anchors the flame, it has been observed its initial strength entrains considerable amounts of reacting species

destabilizing the combustion process, thus generating series of changes in the OH^* production, position of the flame and stability. Therefore, a less intense swirl would be beneficial for such a flame in order to reduce the entrainment of reactive species, increase residence time of products from the methane flame, and extend the interaction between NO_x and the newly formed species from the ammonia cracking process.

Hence, for the purpose of development of practical power generators through fuel flexibility with high hydrogen content fuels [43], these results have demonstrated the strengths and limitations of equilibrium and 1D models for prediction of combustor performance, for example under-predicting unburned fuel and overpredicting CO emissions. A first insight into the influence of ambient pressure has been gained, which enables scaling strategies to be extrapolated towards practical systems, though further experimental validation at elevated pressure is required. Direct application of these medium-pressure results would be of interest to industrial users considering ammonia utilisation in furnaces, for example in the steel industry. Lower swirl number, whilst still retaining vortex breakdown, is likely to be beneficial for flame stability and emission performance, and fully premixed combustion is not the most effective injection strategy for practical applications. Although research is now underway to recognise the potential of ammonia as alternative flexible fuel with focus on new reaction mechanisms for computational studies [44], there is still considerable experimental research to be performed before development of a commercial system is possible.

4. Conclusions

Numerical and experimental studies were carried out to recognise flame stability and emissions parameters in ammonia–methane flames using swirling flows representative of gas turbines. It was observed that the combustion of both molecules causes a complex reaction mechanism that reaches its lowest total emissions – though still unacceptable levels for CO – between 1.15 and 1.25 equivalence ratio. However, stability is compromised as a consequence of the differences in chemical properties in both fuels, recognising that fully premixed combustion using ammonia and methane is not the most effective injection strategy. A stratified methodology of injection needs to be developed to encourage the production of reactive species that can produce water whilst reacting with NO_x to decrease emissions. Numerical 0-D and 1-D codes can be used for guidance. Although predictions over-estimate CO and under-predict NO_x, CO_2 and O_2, the trends can be representative for further development providing an estimate on effects produced from these species at both higher pressure and inlet temperatures. Finally, it is also observed that a medium swirl number can be detrimental to the stability of the flame using ammonia, with a decrease in residence time that would boost further cracking of the NH_3 with less intake of oxygen and reacting radicals. Therefore, a lower swirl number needs to be assessed to improve these characteristics, ensuring that vortex breakdown phenomena are still reached for flame anchoring purposes.

Acknowledgements

The authors gratefully acknowledge the support of Siemens AG in this research. The authors would like to thank all the technical staff at the Gas Turbine Research Centre for their contributions and efforts on this project.

References

[1] Zamfirescu C, Dincer I. Using ammonia as a sustainable fuel. J Power Sources 2008;185:459–65.
[2] Bartels JR. A feasibility study of implementing an ammonia economy. MSc Dissertation, Iowa State University, Iowa: USA; 2008.
[3] Metkemeijer R, Achard P. Ammonia as a feedstock for a hydrogen fuel cell; reformer and fuel cell behaviour. J Power Sources 1994;49:271–82.
[4] Ahlgren W. Fuel power density. ASME J Press Vess Tech 2012;134:054504.
[5] Tallaksen J, Bauer F, Hulteberg C, Reese M, Ahlgren S. Life-cycle greenhouse gas and energy balance of community-scale wind powered ammonia production. NH_3 fuel association; 2014. <https://nh3fuel.files.wordpress.com/2014/10/nh3fa-2014-joel-tallaksen.pdf> [accessed 12.01.15].
[6] Leighty B. NH_3 from renewable-source electricity, water, and air: technology options and economics modelling, greenhouse gas and energy balance of community-scale wind powered ammonia production. NH_3 fuel association; 2014. <https://nh3fuel.files.wordpress.com/2014/10/nh3fa-2014-bill-leighty.pdf> [accessed 12.01.15].
[7] Reese M, Marquart C. Modelling the cost of production of nitrogen fertilizer produced from wind energy. Final report, University of Minnesota, Minnesota: USA; 2010.
[8] Siemer D. Nuclear ammonia – a solution to the world's impending transportation fuel crisis. In: 42nd eng geology geotech eng symp 14th int conf environ: geotech environ energy economics (GE) – links sustain; 2009. p. 189–201.
[9] Varley R, Meyer L, Cooper D. Ocean thermal energy conversion (OTEC). NH_3 fuel association; 2011. <https://nh3fuel.files.wordpress.com/2013/01/2011-varley-meyer-cooper.pdf> [accessed 20.02.15].
[10] Verkamp FJ, Hardin MC, Williams JR. Ammonia combustion properties and performance in gas turbine burners. Int Symp Combust 1967;11(1):985–92.
[11] Pratt DT. Performance of ammonia fired gas turbine combustors. Report TR-9-TS-67-5. Solar San Diego, California: USA; 1967.
[12] Newhall H, Starkman E. Theoretical performance of ammonia as a gas turbine fuel. SAE tech pap 660768; 1966. http://dx.doi.org/10.4271/660768.
[13] Li J, Huang H, Kobayashi N, He Z, Nagai Y. Study on using hydrogen and ammonia as fuels: combustion characteristics and NO_x formation. Int J Energy Res 2014;38:1214–23.
[14] Mathieu O, Petersen EL. Experimental and modelling study on the high-temperature oxidation of ammonia and related NO_x chemistry. Combust Flame 2015;162:554–70.
[15] Ryu K, Zackarakis-Jutz GE, Kong SC. Performance enhancement of ammonia-fueled engine by using dissociation catalyst for hydrogen generation. Int J Hydrog Energy 2014;39:2390–8.
[16] Lear WE. Ammonia-fueled combustion turbines. NH_3 fuel association; 2012. <https://nh3fuel.files.wordpress.com/2012/05/lear_nh3.pdf> [accessed 12.03.15].
[17] Pritchard JD. HPA compendium of chemical hazards: ammonia. Health Protection Agency; 2011.
[18] Karabeyoglu A, Evans B. Fuel conditioning system for ammonia fired power plants. NH_3 fuel association; 2012. <https://nh3fuel.files.wordpress.com/2012/10/evans-brian.pdf> [accessed 10.01.15].
[19] Karabeyoglu A, Evans B, Stevens J, Cantwell B. Development of ammonia based fuels for environmentally friendly power generation. In: 10th annu int energy conver eng conf, IECEC; 2012.
[20] Balestri M, Cecchini D, Cinci V. Unconventional fuels experimental campaigns in gas turbine combustor at ENEL sesta facility. ASME turbo expo; 2004.
[21] Grcar JF, Glarborg P, Bell JB, Loren A, Jensen AD. Effects of mixing on ammonia oxidation in combustion environments at intermediate temperatures. Proc Combust Inst 2003;30(1):1193–200.
[22] Meyer T, Kumar P, Li M, Redfern K, Diaz D. Ammonia combustion with near-zero pollutant emissions. NH_3 fuel association; 2011. <https://nh3fuel.files.wordpress.com/2013/01/2011-meyer.pdf> [accessed 21.02.15].
[23] Ganley J, Bowery MS. Engine-ready, carbon free ammonia fuel. NH_3 fuel association; 2010. <https://nh3fuel.files.wordpress.com/2012/05/afc_2010_ganleyjc_boweryms.pdf> [accessed 20.02.15].
[24] Iki N, Kurata O, Matsunuma T, Inoue T, Suzuki M, Tsujimura T, et al. Micro gas turbine operation with kerosene and ammonia. NH_3 fuel association; 2014. <https://nh3fuel.files.wordpress.com/2014/10/nh3fa-2014-norihiko-iki.pdf> [accessed 10.02.015].
[25] Syred N, Bowen PJ, Sevcenco Y, Marsh R, Morris SM. Preliminary results from a high pressure optical gas turbine combustor model with 3D viewing capability. In: AIAA int meet Orlando; 2015. http://dx.doi.org/10.2514/6.2015-1655.
[26] Runyon J, Marsh R, Valera-Medina A, Giles A, Bowen P. Methane–oxygen flame stability in a generic premixed gas turbine swirl combustor at varying thermal power and pressure. ASME turbo expo. GT2015-43588; 2015.
[27] van Assen HC, Egmont-Petersen M, Reiber JHC. Accurate object localization in grey level images using the centre of gravity measure: accuracy versus precision. IEEE Trans 2002;11:1379–84.
[28] Fritsche D. Origin and control of thermoacoustic instabilities in lean premixed gas turbine combustion. PhD Thesis. Swiss Federal Institute of Technology Zurich: Switzerland; 2005.
[29] Morely C. GASEQ version 0.79; 2010. <http://www.arcl02.dsl.pipex.com> [accessed 25.09.14].
[30] Rutar T, Malte PC. NO_x formation in high-pressure jet-stirred reactors with significance to lean-premixed combustion turbines. J Eng Gas Turb Power 2002;124(3):776–83.
[31] Syred N. A review of oscillation mechanisms and the role of the Precessing vortex core (PVC) in Swirl Combustion systems. Prog Energy Combust Sci 2006;32:93–161.

[32] Valera-Medina A, Syred N, Bowen P. Central recirculation zone visualization in confined swirl combustors for terrestrial energy. J AIAA Propuls Power 2013;29(1):195–204.
[33] Shmakov AG, Korobeinichev OP, Rybitskaya IV, Chernov AA, Knyazkov DA, Bolshova TA, et al. Formation and consumption of NO in $H_2 + O_2 + N_2$ flames doped with NO or NH_3 at atmospheric pressure. Combust Flame 2010;157:556–65.
[34] Duynslaegher C, Jeanmart H, Vandooren J. Ammonia combustion at elevated pressure and temperature conditions. Fuel 2010;89:3540–5.
[35] Duynslaegher C, Contino F, Vandooren J, Jeanmart H. Modelling ammonia combustion at low pressure. Combust Flame 2012;159:2799–805.
[36] Konnov AA. Implementation of the NCN pathway of prompt-NO formation in the detailed reaction mechanism. Combust Flame 2009;156 (11):2093–105.
[37] Perase RWB, Gaydon AG. The identification of molecular spectra. 4th ed. USA: John Wiley & Sons; 1976.
[38] Syred N, Gupta A, Lilley D. Swirl flows. UK: Abacus Press; 1984.
[39] Tian Z, Li Y, Zhang L, Glarborg P, Qi F. An experimental and kinematic modelling study of premixed $NH_3/CH_4/O_2$/Ar flames at low pressure. Combust Flame 2009;156(7):1413–26.
[40] Candel S, Durox D, Schuller T, Bourgouin JF, Moeck JP. Dynamics of swirling flames. Annu Rev Fluid Mech 2014;46:147–73.
[41] Arndt MC, Severin M, Dem C, Stöhr M, Steinberg AM, Meier W. Experimental analysis of thermo-acoustic instabilities in a generic gas turbine combustor by phase-correlated PIV, chemiluminescence, and laser Raman scattering measurements. Exp Fluids 2015;56(4). art 69.
[42] Vigueras Zuniga MO, Valera-Medina A, Syred N, Bowen PJ. High momentum flow region and central recirculation zone interaction in swirling flows. SOMIM 2014;4(6):195–204.
[43] Taamallah S, Vogiatzakia K, Alzahranib FM, Mokheimerb EMA, Habibb MA, Ghoniema AF. Fuel flexibility, stability and emissions in premixed hydrogen-rich gas turbine combustion: technology, fundamentals, and numerical simulations. Appl Energy 2015;154:1020–47.
[44] Nozaria H, Karabeyoğlua A. Numerical study of combustion characteristics of ammonia as a renewable fuel and establishment of reduced reaction mechanisms. Fuel 2015;159:223–33.

Glossary

CoG: Centre of Gravity [pix, pix]
CRZ: central recirculation zone
ER: Equivalence Ratio
FID: Flame Ionisation Detector
G: Gibbs Free Energy [J]
G_i^0: Molar Free Energy at 1 atm for species i [J/mol]
$I(i,j)$: normalised OH^* intensity function [–]
nSp: species n
p: pressure [Pa]
PFR: Plug Flow Reactor
PSR: Perfectly Stirred Reactor
PVC: Precessing Vortex Core
R: Universal Gas Constant [J/mol K]
T: temperature [K]
THC: Total Hydrocarbons
x_i: moles of species i [mol]